Selective aerobic oxidation of biomass derived precursor 5-hydroxymethylfurfural into 2,5-furandicarboxylic acid under mild conditions over a magnetic palladium nanocatalyst

Journal:	*Green Chemistry*
Manuscript ID:	GC-ART-09-2014-001833.R2
Article Type:	Paper
Date Submitted by the Author:	14-Nov-2014

Complete List of Authors:	Zhang, Zehui; South-Central University for Nationalities, key Laboratory of Catalysis and Material Sciences of the State Ethnic Affairs Commission & Ministry of Education Zheng, Judun; South-Central University for Nationalities, key Laboratory of Catalysis and Material Sciences of the State Ethnic Affairs Commission & Ministry of Education Liu, Bing; South-Central University for Nationalities, key Laboratory of Catalysis and Material Sciences of the State Ethnic Affairs Commission & Ministry of Education Lv, Kangle; South-Central University for Nationalities, key Laboratory of Catalysis and Material Sciences of the State Ethnic Affairs Commission & Ministry of Education Deng, Kejian; South-Central University for Nationalities, key Laboratory of Catalysis and Material Sciences of the State Ethnic Affairs Commission & Ministry of Education

Cite this: DOI: 10.1039/c0xx00000x

www.rsc.org/xxxxxx

ARTICLE TYPE

Selective aerobic oxidation of biomass derived precursor 5-hydroxymethylfurfural into 2,5-furandicarboxylic acid under mild conditions over a magnetic palladium nanocatalyst

Zehui Zhang,* Judun Zhen, Bing Liu, Kangle Lv and Kejian Deng

Received (in XXX, XXX) Xth XXXXXXXXX 20XX, Accepted Xth XXXXXXXXX 20XX
DOI: 10.1039/b000000x

In this study, a new method for the highly selective aerobic oxidation of 5-hydroxymethylfurfural (HMF) into 2,5-furandicarboxylic acid (FDCA) is developed by employing a magnetically separable [γ-Fe_2O_3@HAP-Pd(0)] catalyst. The γ-Fe_2O_3@HAP-Pd(0) catalyst was prepared by the exchange of Pd^{2+} with Ca^{2+} in γ-Fe_2O_3@HAP, followed by the reduction of the Pd^{2+} to Pd(0) nanoparticles and well characterized by TEM, XRD and XPS. The as-prepared catalyst showed high catalytic activity for the oxidation of HMF into FDCA in water with high HMF conversion of 97% and FDCA yield of 92.9% under optimal reaction conditions. The developed method demonstrated some superior advantages including the only requirement of the stoichimetric base and high catalytic performance under atmospheric oxygen even in the air. More importantly, the γ-Fe_2O_3@HAP-Pd(0) catalyst could be easily separated from the reaction solution by an external magnetic field and it could be successfully reused five consecutive reaction runs with keeping its catalytic performance. This study shows a green and sustainable method for the production of valuable chemicals from the renewable resources.

Introduction

With the rapid development of world's economy and the declining petroleum reserves, it creates a great pressure to search for renewable resources to produce chemicals and fuels.[1, 2] Unlike other renewable resources, biomass exists as a unique carbon-containing resource.[3] Through biorefinery, the abundant and inexpensive biomass can be converted into useful chemicals and valuable bio-fuels.[4, 5] Therefore, great effort has been devoted to develop various routes for the conversion of biomass into various chemicals and liquid fuels in recent years. [6, 7]

5-Hydroxymethylfurfural (HMF), a heterocyclic furanic molecule substituted in 2,5-position with hydroxyl and aldehyde functionalities, is considered as a promising platform chemical.[8] It can be used as a starting material for the synthesis of functional replacement or direct replacement alternatives to the current commodity chemicals mainly results petrol resources.[9, 10] In recent years, fruitful results have been achieved for the conversion of carbohydrates into HMF in various catalytic systems.[11-13] Currently, there is a growing interest on the subsequent production of value added chemicals from HMF. The catalytic oxidation of HMF (Scheme 1) is one of the most attractive reactions, as several important chemicals can be established via HMF.[14-16] Among them, much more interest has been paid on the oxidation of HMF into 2,5-furandicarboxylic acid (FDCA). On the one hand, FDCA can be widely served as a chemical and medical intermediate.[17] More importantly, FDCA is a promising alternative to petroleum-derived terephthalic acid, which is widely used for the production of key polymers such as polyethylene terephthalate (PET) and polybutyleneterephthalate (PBT) plastics.[18]

Department of Chemistry, Key Laboratory of Catalysis and Material Sciences of the State Ethnic Affairs Commission & Ministry of Education.
South-Central University for Nationalities
MinYuan Road 182, Wuhan, R.P. China
E-mail:zehuizh@mail.ustc.edu.cn

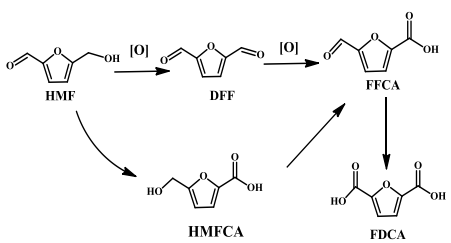

Scheme 1. Possible oxidation products from the oxidation of HMF.

Homogeneous catalytic systems such as $Co^{2+}/Zn^{2+}/Br^-$ and $Co^{2+}/Mn^{2+}/Br^-$ have been reported for the oxidation of HMF into FDCA.[19, 20] One of the main disadvantages of the homogeneous method is that it is difficult to recycle the catalyst, resulting in the serious environmental pollution and high cost in production. Therefore, the use of heterogeneous catalyst has been attracted great interest in the oxidation of HMF into FDCA, which overcomes the above mentioned drawbacks of homogeneous catalysts. Supported Au nanoparticles have been shown encouraging catalytic performances for the aerobic oxidation of HMF to FDCA in water. For example, Corma et al. reported that CeO_2-supported Au nanoparticles (CeO_2/Au) showed high catalytic activity for the oxidation of HMF to FDCA with high yield of 99% at 130 ^oC under 1 MPa air pressure and high concentration of NaOH (4 equiv of HMF).[21] Davis et al. reported that 100% HMF conversion and 65% FDCA yield were obtained by the use of high NaOH/HMF mole ratio of 20 over Au/TiO_2 catalyst under 345 kPa oxygen pressure.[22] Xu et al., improved the method of the oxidation of HMF into FDCA with supported Au catalyst. They found that gold nanoclusters confined in a supercage of Y zeolite showed high catalyst activity and selectivity for aerobic oxidation of HMF into FDCA with NaOH/HMF mole ratio of 3 under 5 bar oxygen.[23] Besides supported Au nanoparticles, other supported metal nanoparticles such as Pt [22] and Pd [24] have also been studied for the aerobic oxidation of HMF into FDCA. For example, Davis et al. [24] directly compared supported Au, Pd, and Pt catalysts and found that Pd/C and Pt/C were more selective towards FDCA (71–79%) than Au/C at complete HMF conversion under identical conditions (6 h, 1 : 2 molar ratio HMF–KOH, 7 bar O_2, 295 K). Taking all these reported methods into consideration, these developed methods showed some drawbacks such as the instability of the catalysts and the use of large amount of base and the requirement of high oxygen pressure. Therefore, it is still strongly demanded to develop highly active and stable heterogeneous catalysts for highly efficient oxidation of HMF to FDCA under mild conditions.

Recently, magnetic catalysts have been received great attention in liquid chemical reactions, as magnetic catalysts can be simply removed from the reaction system by magnetic separation.[25] However, it requires tedious recovery procedure *via* filtration or centrifugation to recover common heterogeneous catalyst, which sometimes results in the loss of solid catalysts. Hydroxyapatite-encapsulated magnetic γ-Fe_2O_3 (γ-Fe_2O_3@HAP) nanocrystallities have been recently used as high-performance heterogeneous catalytic supports for different kinds of chemical reactions.[26, 27] More importantly, the Ca^{2+} in the shell layer of HAP can be exchanged with other metal cations, thus it can introduce various active sites for many chemical reactions. Recently, we have found that ruthenium-exchanged hydroxyapatite encapsulated magnetic γ-Fe_2O_3 (γ-Fe_2O_3@HAP-Ru) showed high catalytic for the oxidation of HMF into 2, 5-diformylfuran (DFF) in toluene.[28] In continuation of our previous work, and the aim to develope enriomental-friendly method for the converion of biomass derived HMF into more valuable chemicals in mind, in the present study, γ-Fe_2O_3@HAP supported Pd nanoparticles were prepared and it was found to show high catalytic activity for the oxidation of HMF into FDCA in water under mild conditions. To the best of our knowledge, this is the first time to use the magnetic catalyst for the highly efficient and selective aerobic oxidation of HMF into FDCA in water under atmospheric oxygen pressure by the use of low dosage of K_2CO_3 (0.5 equiv mole ratio of HMF).

Experimental Section

Materials

$FeSO_4.7H_2O$, $FeCl_3.6H_2O$, $Ca(NO_3)_2$ $4H_2O$, $(NH_4)_2HPO_4$, K_2CO_3, sodium tetrahydroborate ($NaBH_4$) and all solvents were purchased from Sinopharm Chemical Reagent Co., Ltd. (Shanghai, China). Sodium tetrachloropalladate(II) (Na_2PdCl_4) was purchased from Aladdin Chemicals Co. Ltd. (Beijing, China). HMF (98%) was purchased by Beijing Chemicals Co. Ltd. (Beijing, China). DFF and FDCA were purchased from the J&K Chemical Co. Ltd., (Beijing, China). Acetonitrile (HPLC grade) was purchased from Tedia Co. (Fairfield, USA). All the above reagents were used as received without further purification. Ultrapure water was used for the catalyst preparation and catalytic reactions.

Catalyst synthesis

Synthesis of γ-Fe_2O_3@HAP-Pd^{2+}

γ-Fe_2O_3@HAP was prepared and characterized as reported in our previous work.[28] The cation-exchange of Ca^{2+} in γ-Fe_2O_3@HAP with Pd^{2+} was described as follows: Finely powdered γ-Fe_2O_3@HAP (0.4 g) was added into a solution of Na_2PdCl_4 (30 mg) in 30 ml of H_2O, and the mixture was stirred at room temperature for 12 h. Then the γ-Fe_2O_3@HAP-Pd^{2+} sample was separated by a permanent magnet, washed with deionized water (40 mL) three times, and dried at 50 ^oC in a vacuum oven overnight.

Synthesis of γ-Fe_2O_3@HAP-Pd(0)

γ-Fe_2O_3@HAP-Pd^{2+} (200 mg) was homogeneously dispersed in ethanol (20 mL) by ultrasonication. Then freshly prepared solution of $NaBH_4$ (22.5 mg) in 10 mL of ethanol was added into the mixture dropwise with a vigorous stirring. The color of the mixture immediately changed from brown to dark, which indicated that the Pd nanoparticles were formed after the addition of $NaBH_4$. After the complete addition of $NaBH_4$, the mixture was further stirred for 6 h at room temperature. Then the γ-Fe_2O_3@HAP-Pd(0) catalyst was collected by an external magnet, and washed with deionized water (40 mL) three times, and dried at 30 ^oC under vacuum overnight.

Catalyst characterization

Transmission electron microscope (TEM) images were performed on an FEI Tecnai G^2-20 instrument. The sample powder were firstly dispersed in ethanol and dropped onto copper grids for observation. X-ray powder diffraction (XRD) patterns of samples were determined with a Bruker advanced D8 powder diffractometer (Cu Kα). All XRD patterns were collected in the

2θ range of 10–80° with a scanning rate of 0.016°/s. X-ray photoelectron spectroscopy (XPS) was conducted on a Thermo VG scientific ESCA MultiLab-2000 spectrometer with a monochromatized Al Kα source (1486.6 eV) at constant analyzer pass energy of 25 eV. The binding energy was estimated to be accurate within 0.2 eV. All binding energies (BEs) were corrected referencing to the C1s (284.6 eV) peak of the contamination carbon as an internal standard. The Pd content in the γ-Fe_2O_3@HAP-Pd(0) catalyst was quantitatively determined by inductively coupled atomic emission spectrometer (ICP-AES) on an IRIS Intrepid II XSP instrument (Thermo Electron Corporation).

Typical procedure for the aerobic oxidation of HMF

Typically, HMF (0.4 mmol, 50.4 mg) was firstly dissolved in water (8 mL) in a 25 mL two-neck round-bottom flask at room temperature with a magnetic stirring at a constant rate of 600 revolutions per minute (rpm). Then γ-Fe_2O_3@HAP-Pd(0) catalyst (40 mg) and K_2CO_3 (0.2 mmol, 27.6 mg) were added quickly into the HMF solution. Then oxygen was flowed at a rate of 20 mL min^{-1} from the bottom of the reactor through one neck, and the other neck of the round bottom was equipped with reflux condenser to avoid the solvent evaporation from the reaction system. Then the reactor was immersed into a pre-heating oil-bath and the reaction was carried out the designed reaction temperature with a magnetic stirring at 600 rpm. Time zero was recorded after the reactor immersed in the oil-bath. After reaction, the γ-Fe_2O_3@HAP-Pd(0) catalyst was separated from the reaction mixture by a permanent magnet, and the liquid solution was diluted to a certain volume to be analyzed by HPLC method.

As far as the use of oxygen balloon reaction, the air in the reactor was exchanged with oxygen three times, and then pure oxygen was filled in the reactor with an oxygen balloon under atmospheric pressure. As far as the reaction in air, the reactor was directly exposed in the air. Other reaction conditions were the same as described above.

Analytic Methods

Products analysis was performed on a ProStar 210 HPLC system. Furan compounds including HMF, FDCA, DFF and HMFCA could be successfully separated by a reversed-phase C18 column (200 × 4.6 mm). The amount of furan compounds was sensitive to UV detector at a wavelength of 280 nm. The mobile phase was composed of acetonitrile and 0.1 wt.% acetic acid aqueous solution with the volume ratio of 30:70, and the flow rate was 1.0 mL/min. The retention time of HMF, FDCA, FFCA, DFF and HMFCA were 3.0 min, 2.6 min, 2.9 min, 3.5 min and 3.7 min, respectively.

The content of HMF, DFF and FDCA in samples were obtained directly by interpolation from calibration curves.

HMF conversion, DFF and FDCA yields are calculated as follows:

HMF conversion = moles of HMF/moles of starting HMF ×100%

FDCA yield = moles of FDCA/moles of starting HMF ×100%

DFF yield = moles of DFF/moles of starting HMF ×100%

Recycling of the catalyst

After reaction, the γ-Fe_2O_3@HAP-Pd(0) catalyst was collected by a permanent magnet, and washed with a large amount of water until the solution was neutral, followed by ethanol. The spent catalyst was then dried under vacuum at 50 °C overnight. The spent catalyst was reused for the next cycle, and other steps were the same as described for the first run.

Results and Discussion

Catalyst preparation and characterization

The procedure of the synthesis of γ-Fe_2O_3@HAP-Pd(0) catalyst is illustrated in Scheme 2. The support γ-Fe_2O_3@HAP was prepared and characterized as described in our previous work.[28] Briefly, co-precipitation of Fe^{2+} and Fe^{3+} ions in alkaline solution under nitrogen atmosphere produced Fe_3O_4 nanoparticles. Fe_3O_4 nanoparticles were then coated with HAP, which was formed from Ca^{2+} and PO_4^{3-} at pH=11. Then the as-prepared material was then calcined at 300 °C for 3 h to produce γ-Fe_2O_3@HAP. γ-Fe_2O_3@HAP-Pd^{2+} was prepared by the cation exchange of Ca^{2+} in γ-Fe_2O_3@HAP with Pd^{2+}, which was a brown powder. Then, Pd^{2+} was reduced by $NaBH_4$ in ethanol to generate the γ-Fe_2O_3@HAP-Pd(0) catalyst. After addition of $NaBH_4$, the color of the catalyst immediately changed from brown to dark grey, which indicated Pd^{2+} in γ-Fe_2O_3@HAP-Pd^{2+} was successfully reduced to Pd(0) nanoparticles. The content of Pd was determined to be 2.5 wt.% by ICP-AES analysis.

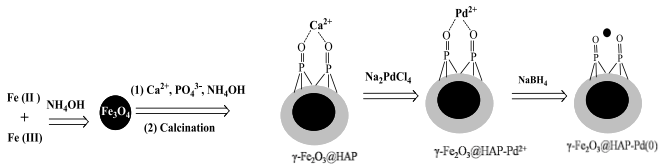

Scheme 2 Schematic illustration of the preparation of the γ-Fe_2O_3@HAP-Pd(0) catalyst

TEM images of the fresh γ-Fe_2O_3@HAP-Pd(0) catalyst and the spent γ-Fe_2O_3@HAP-Pd(0) catalyst are shown in Fig. 1. Seeing from Fig. 1 (a), the fresh catalyst shows the presence of homogeneously distributed palladium nanoparticles with sphere morphology on the surface of γ-Fe_2O_3@HAP. Such sphere palladium nanoparticles have also been observed on both HAP supported $Pd(OAc)_2$ and $PdCl_2(MeCN)_2$ after reduction.[29, 30] It is worth noting that there is almost no difference in the TEM images between the fresh catalyst and spent catalyst (Fig. 1(a) *vs* Fig. 1(b)). After reused for five times, palladium nanoparticles still homogeneously distributed on the surface of γ-Fe_2O_3@HAP (Fig. 1b), and no apparent aggregation of the palladium nanoparticles was observed.

The particle size distribution histograms of Pd nanoparticles of the fresh catalyst and the spent catalyst are shown in Fig. 2. There is no apparent difference in the size distribution of Pd nanoparticles between the fresh catalyst and the spent catalyst. The average particle sizes of the fresh catalyst and the spent catalyst were almost the same at 2.8 nm, and 2.9 nm, respectively.

That is the reason why the γ-Fe_2O_3@HAP-Pd(0) catalyst shows no significant loss of its catalytic activity during the catalyst recycling experiments (as shown in Fig. 8). By the way, some bulk black area was also observed in the TEM images, which was due to the aggregation of γ-Fe_2O_3 during the formation of γ-Fe_2O_3@HAP as described in our previous work. [28]

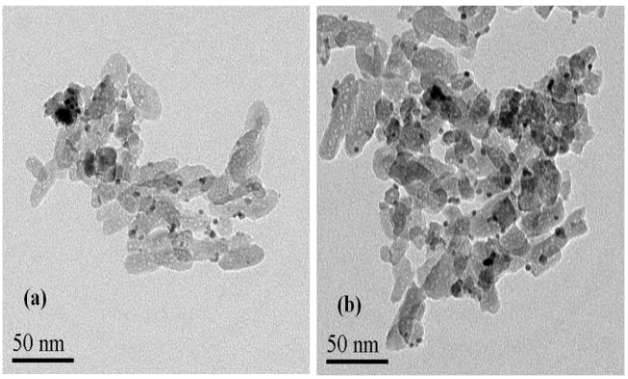

Fig. 1 TEM images of the γ-Fe_2O_3@HAP-Pd(0) catalyst (a) fresh; (b) spent catalyst after six cycles.

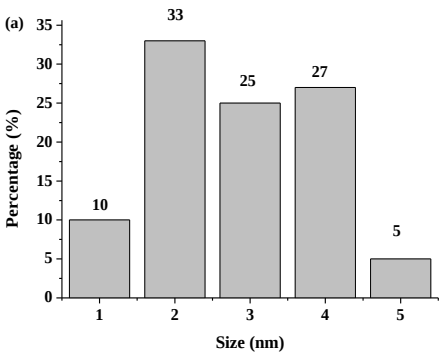

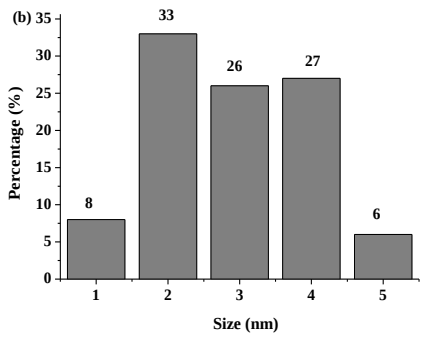

Fig. 2 The particle size distribution histograms of Pd nanoparticles (a) the fresh catalyst and (b) the spent catalyst.

XRD patterns of the as-prepared γ-Fe_2O_3@HAP-Pd(0) catalyst is shown Fig. 3. These peaks with 2θ = 35.7°, 43.6°, 53.6°, 57.4° and 63.1° are attributed to the γ-Fe_2O_3, which matches well with the standard reflection peaks of γ-Fe_2O_3 (JCPOS card no. 25-1402).[26] HAP also shows its typical diffraction peaks with 2θ = 25.8°, 31.7°, 32.8°, 34.2°, 39.8°, 46.8°, and 49.5°.[26] The intensity of the signal at 39.8° was approximately 1/5 of the intensity of the peak at about 32.8° C which corresponds to the intensity ratio of HAP signals at both angles (PDF-2-No. [084-1998] (ICDD)). It is reported that Pd(0) also exhibits three diffraction peaks with 2θ observed at 40.1°, 46.5° and 68.1° (ref. JCPDS file: 46–1043).[31]. The peaks at 46.5° and 68.1° might overlap with the peaks presented in HAP. However, the peak at 68.1° was not observed, These results indicated that there were no Pd(0) peaks in Fig. 3. The possible reason should be attributed to the following two aspects. On the one hand, the loading of Pd was low in the catalysts. On the other hand, the particle size of Pd was quite small, resulting homogeneous granules dispersion, as the TEM results indicated that the average of particle size was estimated to be 2.8 nm for the prepared catalyst, respectively.[32]

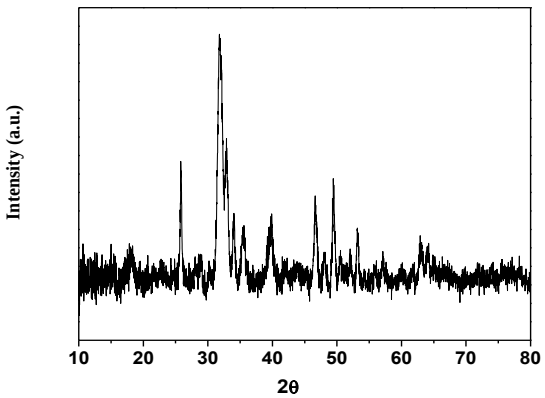

Fig. 3 XRD patterns of the γ-Fe_2O_3@HAP-Pd(0) catalyst.

To further gain the insights into the surface element composition and valence state of the catalyst, the catalyst was further characterized by XPS technology. Fig. 4 (A) presents the XPS elementary survey scans of surface elemental composition in the γ-Fe_2O_3@HAP-Pd(0) catalyst. These peaks corresponding to oxygen, calcium, phosphorus, palladium elements are clearly observed. Weak peaks with the binding energy at 710.9 and 724.1 eV are also observed in Fig. 4 a, which correspond the binding energy of Fe $2p_{3/2}$ and Fe $2p_{1/2}$, respectively. The XPS results indicate that some Fe_2O_3 particles were not successfully encapsulated by HAP. These Fe_2O_3 particles were most probably to be the black areas in TEM, caused by the aggregation of Fe_2O_3 particles. The XPS results of element Pd in γ-Fe_2O_3@HAP-Pd^{2+} and γ-Fe_2O_3@HAP-Pd(0) are shown in Fig. 4 (b) and (c), respectively. Two peaks appeared at 337.8 eV and 341.5 eV in γ-Fe_2O_3@HAP-Pd^{2+} are assigned to Pd $3d_{3/2}$ and Pd $3d_{5/2}$, which are the characteristic 3d peaks of Pd^{2+}.[33] These results indicate that Pd^{2+} was partially exchanged with the Ca^{2+} in γ-Fe_2O_3@HAP. After the reduction of γ-Fe_2O_3@HAP-Pd^{2+} by $NaBH_4$, the corresponding Pd 3d region is shown in Fig. 4 c. Pd $3d_{3/2}$ and Pd $3d_{5/2}$ peaks with the binding energy at 335.1 eV and 340.4 eV are the characteristic 3d peaks of Pd(0) nanoparticles in agreement with the results reported by others.[33] The XPS results clearly verify that the Pd^{2+} in γ-Fe_2O_3@HAP-Pd^{2+} was reduced to Pd(0) in the presence of $NaBH_4$. However, the peaks with the binding energy at 337.7 eV and 341.5 eV peak were also observed, and the two peaks are assigned to Pd $3d_{3/2}$ and Pd $3d_{5/2}$ respectively. As the $NaBH_4$ amount was 10 times of Pd^{2+}, the presence of the

Pd^{2+} should be attributed to the oxidation of Pd(0) during the storage. In fact, some authors also claimed that the metal(0) nanoparticles could be oxidized to high valence state metal oxide.[34]

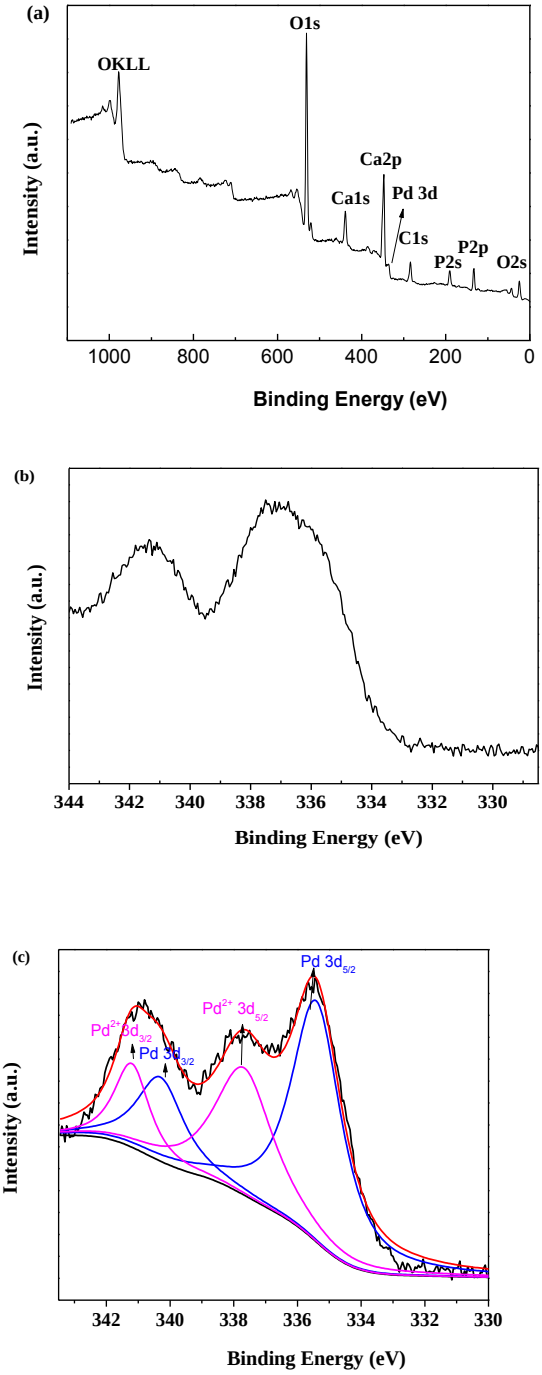

Fig. 4 XPS spectra of the samples. (a) Survey scan of γ-Fe_2O_3@HAP- Pd(0); (b) Pd^{2+} 3d region in $NaPdCl_4$; (c) Pd(0) 3d region in γ-Fe_2O_3@HAP- Pd(0) catalyst .

Aerobic oxidation of HMF in various solvents

Table 1. The results of HMF oxidation in different solvents.[a]

Entry	Solvent	$\varepsilon/\varepsilon_0$[35]	HMF conversion (%)	FDCA yield (%)	DFF yield (%)
1	Toluene	2.38	9.4	0	7.4
2	4-Chlorotoluene	6.1	8.4	0	6.2
3	Ethanol	24.5	10.4	6.4	3.1
4	DMSO	46.7	14.2	7.2	3.9
5	H_2O	80.1	21.2	13.2	7.2
6[b]	H_2O	80.1	100	51.6	0

[a] Reaction conditions: HMF (50.4 mg, 0.4 mmol), solvent (8 mL), γ-Fe_2O_3@HAP-Pd(0) (40 mg), oxygen flow rate (30 mL min^{-1}), 100 ^oC, 6 h.
[b] K_2CO_3 (0.4 mmol) was used, and otherwise conditions were the same as described above.

Generally speaking, the properties of the solvent such as the polarity, dielectric constant, steric hindrance, acid-base property show great effect on the chemical reaction.[36] Therefore, the aerobic oxidation of HMF over γ-Fe_2O_3@HAP-Pd(0) catalyst was initially carried out in various solvents to study to the solvent effect. Table 1 shows the results of HMF aerobic oxidation in each solvent as well as the dielectric constants of the solvents used. The dielectric constant (or relative permittivity) is a relative measure of the solvent polarity. As shown in Table 1, the solvent greatly affected HMF conversion and product selectivity. DFF was only formed in aromatic solvent such as toluene and 4-chlorotoluene (Table 1, Entries 1 & 2). FDCA has a high dielectric constant (or polarity), which is insoluble in the solvent with low dielectric constant. Therefore, we could not get FDCA by the oxidation of HMF in toluene and 4-chlorotoluene. It is interesting to find that HMF conversion and DFF yield in toluene was slightly higher than those obtained in 4-chlorotoluene. It is possible due to the higher solubility of oxygen in toluene than 4-chlorotoluene (oxygen is a non-polar molecule) .[37]

FDCA and DFF were simultaneously produced when the oxidation of HMF was carried out in polar solvent with large dielectric constant such as ethanol, dimethyl sulfoxide (DMSO) and water (Table 1, Entries 3-5). Besides, HMFCA was also detected as an intermediate, but in a very low content. Interestingly, it is worth noting that both HMF conversion and products yields increased with an increase of the solvent polarity. The highest HMF conversion of 21.2% was obtained in water, and FDCA and DFF yields were 13.2% and 7.2%, respectively (Table 1, Entry 5). The oxidation of HMF using water as green solvent with molecular oxygen as the oxidant appears very appealing due to its low cost and without toxic pollution albeit

the catalytic activity of γ-Fe_2O_3@HAP-Pd(0) was not very high under the present reaction conditions. Based on the fact that the addition of base usually promotes the conversion of HMF into FDCA using supported Au nanoparticles as catalysts,[21-23] the aerobic oxidation of HMF in water over γ-Fe_2O_3@HAP-Pd(0) catalyst was further carried out by the addition of 1 equiv of K_2CO_3 (based on HMF mole value). To our delights, HMF conversion of 100% and FDCA yield up to 51.6% were obtained under otherwise the same conditions (Table 1, Entry 6). The results from Entry 5 and Entry 6 indicated that K_2CO_3 accelerated the transformation of HMF into FDCA. Detail results on the effect of base amount on the oxidation of HMF were further studied in the following section.

Effect of the base amount on the aerobic oxidation of HMF into FDCA

Table 2. The results of aerobic oxidation of HMF using different amount of K_2CO_3. [a]

Entry	Mole ratio of K_2CO_3 to HMF	HMF conversion (%)	FDCA yield (%)	FDCA selectivity (%)
1	1	100	51.6	51.6
2	0.75	100	78.9	78.9
3	0.5	97	92.9	95.7
4	0.37	80.4	76.1	94.1
5	0.25	63.8	60.5	95.0
6	0.125	36.8	27.1	73.6
7	0	21.2	13.2	7.2

[a] Reaction conditions: HMF (50.4 mg, 0.4 mmol), H_2O (8 mL), γ-Fe_2O_3@HAP-Pd(0) (40 mg), a set amount of K_2CO_3, oxygen flow rate (30 mL min^{-1}), 100 °C, 6 h.

As discussed above, K_2CO_3 indeed played a positive role in the oxidation of HMF in water over γ-Fe_2O_3@HAP-Pd(0) catalyst. To further optimize the reaction conditions, the effect of K_2CO_3 dosage on the aerobic oxidation of HMF was studied. As shown in Table 2, it is clearly observed that the oxidation of HMF is very sensitive to K_2CO_3. Quantitative HMF conversion was obtained by the use of 1 equiv of K_2CO_3 (Table 2, Entry 1). However, the yield of FDCA was only 51.6%, and no other furan compounds such as DFF were detected (Table 2, Entry 1). The possible reason should be that HMF is not stable under alkaline condition especially at a relative high reaction temperature of 100 °C. In fact, HMF was subjected to be heated in the presence of 1 equiv of K_2CO_3. As expected, the degradation ratio of HMF reached 49.2%. Our results matched well with the results reported by Rass et al.[38] They also found that the treatment of Na_2CO_3 (2 equiv) aqueous solution of HMF at 100 °C yielded 50% HMF degradation after 2 h. Therefore, in order to reduce the degradation of HMF and improve FDCA selectivity, experiments of the oxidation of HMF were carried out by the gradual decrease of K_2CO_3 amount. As shown in Table 2, decreasing the mole ratio of K_2CO_3/HMF from 1 to 0.5 showed no significant effect on HMF conversion, but HMF yield greatly increased from 51.6% to 94.1% (Table 2, Entries 1 ~3). The reason was that less HMF was degraded with less amount of K_2CO_3. In addition, the reaction solution after 6 h was obviously alkaline by the use of 1 equiv and 0.75 equiv of K_2CO_3, while the pH value (7.4) of the reaction solution was close to neutral by the use of 0.5 equiv of K_2CO_3. 0.5 equiv of K_2CO_3 is the stoichiometric amount to neutralize the formed FDCA in theory. Thus, on the one hand, 0.5 equiv of K_2CO_3 is enough to neutralize the theoretical amount of FDCA, which avoids FDCA to coat on the surface of Pd nanoparticles and keeps the catalyst activity. On the other hand, the serious degradation of HMF can also be inhibited as the concentration of K_2CO_3 is not high, most of which is used to neutralize FDCA.

Further decreasing the mole ratio of K_2CO_3/HMF from 0.37 to 0.125, HMF conversion and FDCA yield gradully decreased (Table 2, Entries 4~6). As expected, when the dosage of K_2CO_3 was low than 0.5 equiv, K_2CO_3 was consumed by reaction with the formed FDCA, resulting in the cease of the promotion the oxidation of HMF. It is worth noting that HMF oxidation over γ-Fe_2O_3@HAP-Pd(0) was very sluggish in the absence of K_2CO_3 (Table 2, Entry 7). Taking all the above results into consideration, the role of the K_2CO_3 is that it is used to neutralize the strong adsorption of carboxylic acids formed on the catalyst surface, thus keeping the metal catalyst to be active during the reaction process.[39]

Aerobic Oxidation of HMF into FDCA using common alkaline species

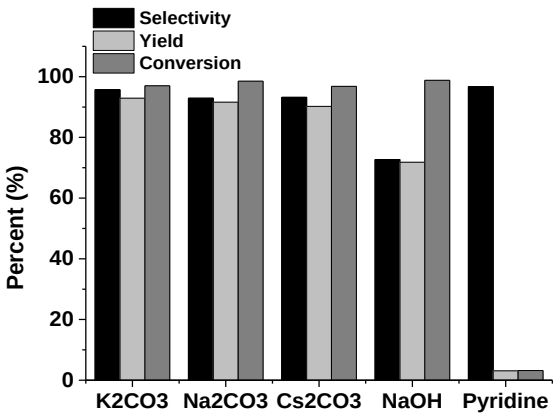

Fig. 5 The results of HMF oxidation in water in the presence of various bases. Reaction conditions: HMF (50.4 mg, 0.4 mmol), H_2O (8 mL), γ-Fe_2O_3@HAP-Pd(0) (40 mg), K_2CO_3 (27.6 mg, 0.2 mmol), oxygen flow rate (30 mL min^{-1}), 100 °C, 6 h. [b] For the use of NaOH and pyridine, 1 equiv was used.

To further study the effect of base on the oxidation of HMF in water over γ-Fe_2O_3@HAP-Pd(0) catalyst, the impact of various bases such as CO_3^{2-} base, NaOH and organic base (pyridine) was also studied, and the results are shown in Fig. 5. It is noted that the CO_3^{2-} base with different alkali metals almost showed no difference in the oxidation of HMF. Similar HMF conversion and FDCA yield were obtained by the use of K_2CO_3, Na_2CO_3 and Cs_2CO_3. Although high HMF conversion of 98.8% was also observed by the use of NaOH, low FDCA yield of 71.8% was obtained. The reason should be the same as we discussed above for the use of 1 equiv of K_2CO_3. NaOH is a strong base, while the base strength of CO_3^{2-} base is much weaker with pK_b value of 3.65.[40] Therefore, much more HMF would be degraded when using 1 equiv of NaOH, resulting in low FDCA selectivity. It is observed that both HMF conversion and FDCA yield were low about 3% when organic base pyridine was used. On the one hand, the base strength of pyridine is too weak to react with the carboxylic acid groups of FDCA. On the other hand, nitrogen-containing organic bases such as quinoline and pyridine have strong coordination ability with Pd nanoparticles.[41] In fact, Lignier et al., found that the heterocyclic amines were inferior solvents for the Au/TiO_2-catalyzed aerobic epoxidation of stilbene this reaction.[42] Therefore, strong interaction between pyridine and the Pd nanoparticles might also be responsible for the weak catalytic activity of γ-Fe_2O_3@HAP-Pd(0) on the oxidation of HMF into FDCA.

Effect of reaction temperature on the aerobic oxidation of HMF into FDCA

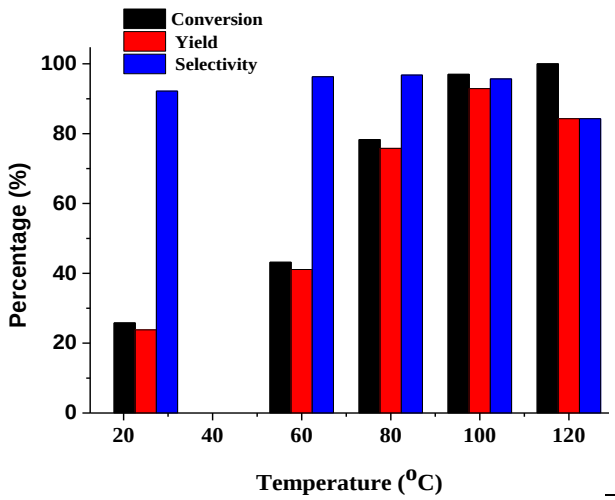

Fig. 6 The results of the oxidation of HMF over γ-Fe_2O_3@HAP-Pd(0) at different reaction temperature. Reaction conditions: HMF (50.4 mg, 0.4 mmol), H_2O (8 mL), γ-Fe_2O_3@HAP-Pd(0) (40 mg), K_2CO_3 (27.6 mg, 0.2 mmol), oxygen flow rate (30 mL min^{-1}), 6 h.

The effect of the reaction temperature on the oxidation of HMF was studied under otherwise the same reaction conditions. Experiments were conducted at five different temperatures between 25 and 120 °C to study the effect of temperature on HMF conversion and FDCA selectivity. It is clear seen from Fig. 5 that the reaction temperature showed a remarkable influence on the oxidation of HMF into FDCA. An increase in the HMF conversion and FDCA yield was observed when the reaction temperature was raised from 25 to 100 °C. For example, HMF conversion and FDCA yield were 25.8% and 23.8% after 6 h at 25 °C, respectively, while those were 97.0% and 92.9% at 100 °C, respectively. However, there was practically no difference in FDCA selectivity at the reaction temperature between 25 and 100 °C. Further increasing the reaction temperature to 120 °C, full HMF conversion was obtained after 6 h. However, FDCA was obtained in a low yield of 84.3%. The possible reason should be that HMF degradation became much more serious at high reaction temperature, resulting in the decrease of the FDCA selectivity. Therefore, 100 °C is the optimal reaction temperature for the oxidation of HMF in water over γ-Fe_2O_3@HAP-Pd(0) catalyst with 0.5 equiv of K_2CO_3, which not only keeps the catalyst with high activity but also does not cause the apparent degradation of HMF.

Effect of oxygen pressure on the oxidation of HMF into FDCA

Table 3. The results of HMF oxidation under different oxygen conditions. [a]

Entry	Time (h)	Condition	HMF conversion (%)	FDCA yield (%)	FDCA selectivity (%)
1	6	O_2	97	92.9	95.7
2	6	O_2 balloon	67.1	63.2	94.2
3	12	O_2 balloon	92.1	83.0	90.1
4	6	In the air	45.6	42.1	92.3
5	12	In the air	83.0	74.2	89.4
6[b]	6	O_2	62.4	56.6	90.7

[a] Reaction conditions: HMF (50.4 mg, 0.4 mmol), H_2O (8 mL), γ-Fe_2O_3@HAP-Pd(0) (40 mg), K_2CO_3 (27.6 mg, 0.2 mmol), 100 °C.
[b] HMF (100.8 mg, 0.8 mmol) was used under otherwise the same reaction conditions as Entry 1.

The high catalytic activity of γ-Fe_2O_3@HAP-Pd(0) on the oxidation of HMF in water with the flow of O_2 promoted us to carry out this reaction under much milder reaction conditions. Instead of the flow of O_2, experiments were also performed by the use of O_2 balloon and in the air, and the results are summarized in Table 3. According to the results from Entries 1, 2, and 4, it is observed that HMF conversion and FDCA yield decreased gradually in an order of O_2 flow, O_2 balloon, and in the air. That was due to the O_2 concentration in the reaction solution gradually decreased under the reaction conditions in Entries 1, 2, and 4, which was consistent with the trend noted by Casanova et al. with oxygen pressure between 100 kPa and 1000 kPa on the

oxidation of HMF into FDCA over their Au/CeO_2.[21] These results clearly indicated that O_2 as one of the reactant determined the oxidation rate of HMF. By the way, the selectivity of FDCA was almost not affected by the O_2 concentration. As shown in Table 3, Entries 3 & 5, good results could also be obtained when the flow of O_2 was replaced with an oxygen balloon or direct in the air after prolonging the reaction time from 6 h to 12 h. To the best of our knowledge, such a high catalytic activity in the liquid-phase oxidation of HMF in water by the use of stoichiometric amount of K_2CO_3 under atmospheric pressure of O_2 using supported palladium catalysts has not yet been reported.

In addition, we have tried to increase the content of the substrate HMF. Therefore, we have carried out the aerobic oxidation of HMF with 0.8 mmol of HMF under otherwise the same reaction conditions by the use of 0.4 mmol of HMF as the substrate. Compared the results in Entry 1 and Entry 6, HMF conversion of 62.4% and FDCA yield of 56.6% were obtained (Table 2, Entry 8). The reason was that K_2CO_3 was not enough to neutralize the produced FDCA.

Effect of catalyst loading on the oxidation of HMF into FDCA

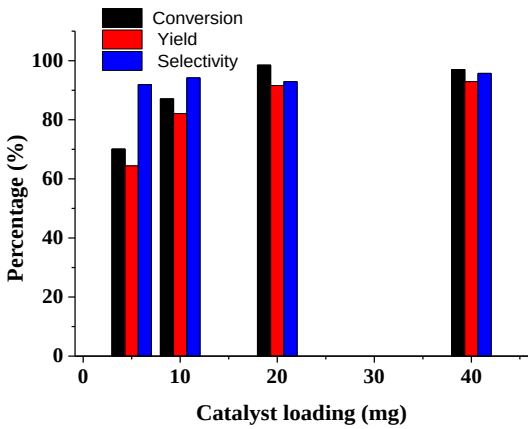

Fig. 7 The results of HMF oxidation by the use of different catalyst loading. Reaction conditions: HMF (50.4 mg, 0.4 mmol), H_2O (8 mL), a set amount of γ-Fe_2O_3@HAP-Pd(0), K_2CO_3 (27.6 mg, 0.2 mmol), O_2 at a flow rate of 30 mL min^{-1},100 ^oC, 6 h.

The aerobic oxidation of HMF was also carried out with different amount of γ-Fe_2O_3@HAP-Pd(0) to investigate the effect of catalyst loading on the oxidation of HMF while keeping other operating conditions constant. HMF conversion and FDCA yield as a function of the catalyst amount is represented in Fig. 7. As discussed above, FDCA can not be produced by the oxidation of HMF without catalyst. However, good HMF conversion of 70.1% and FDCA yield of 64.4% were obtained after 6 h by the use of a little amount of γ-Fe_2O_3@HAP-Pd(0) (5 mg). These results indicated the Pd nanoparticels were very active for the aerobic oxidation of HMF. Further increasing the catalyst loading from 5 mg to 20 mg, HMF conversion and DFF yield increased gradully with the increase of the catalyst loading at the same reaction time point. HMF conversions reached 87.1% and 98.5% after 6 h by the use of 10 mg and 20 mg of γ-Fe_2O_3@HAP-Pd(0), respectively, and the corresponding FDCA yields were 82.1% and 94.2%, respectively. The increase of HMF conversion with an increase of the catalyst amount at the same reaction time period should be attributed to an increase in the availability and number of catalytically active sites. Further increasing the catalyst amount to 40 mg, HMF conversion and FDCA yield did not changed siginificantly. The results indicates that the catalytic sites of 20 mg of γ-Fe_2O_3@HAP-Pd(0) was enough to absorb the substrate HMF to promote the oxidation reaction. It is worth noting that the selectivity of FDCA with different catalyst loading was almost the same. It seems that the product selectivity has no direct relationship with the catalyst amount, as the examined reactions were carried out under otherwise the identical reaction conditions such as reactionn temperature, base concentration.

Recycling experiments

Fig. 8 Recycle of the catalyst by an external magnet.

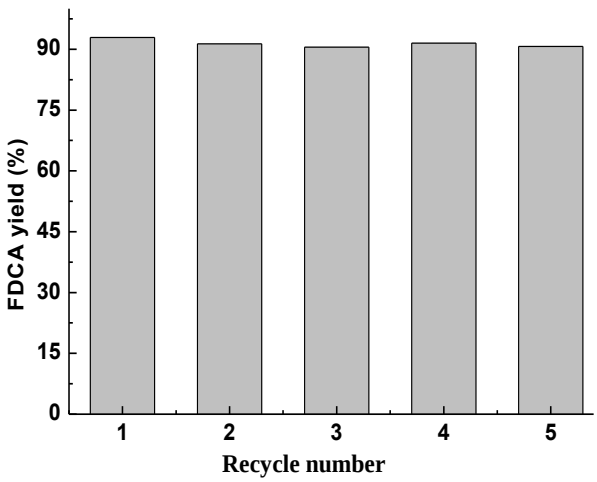

Fig. 9 Stability test for the γ-Fe_2O_3@HAP-Pd(0) catalyst. Reaction conditions: HMF (50.4 mg, 0.4 mmol), H_2O (8 mL), γ-Fe_2O_3@HAP-Pd(0) (40 mg), K_2CO_3 (27.6 mg, 0.2 mmol), O_2 at a flow rate of 30 mL min^{-1},100 ^oC, 6 h.

For the use of the heterogeneous catalyst, one important point is the stability and recyclability of the catalyst. Therefore, recycle of the γ-Fe_2O_3@HAP-Pd(0) catalyst was studied. After the first run, the catalyst was quantitatively separated from the reaction mixture by an external magnet (as shown in Fig. 8). The spent catalyst was thoroughly washed with water and ethanol in sequence, and reused in subsequent runs under identical reaction conditions. As shown in Fig. 9, FDCA yield was almost the same after five runs (92.9% yield in the first run; 90.7% yield in the fifth run). These results demonstrated that there was no significant change in the activity of γ-Fe_2O_3@HAP-Pd(0) up to the 5th use. The reaction solution was subjected to be analyzed by ICP, and no leach of Pd was detected in the reaction solution. In addition, as shown in Fig. 1 and 2, it is observed that the catalyst exhibited almost no morphological changes as evidenced by comparison of TEM images before and after catalysis. According to the above two analysis of the spent catalyst, it is easily to understand the high stability of our prepared γ-Fe_2O_3@HAP-Pd(0) in the oxidation of HMF into FDCA. However, it should point out that there was still a very little decrease of FDCA yield between the first run and the fifth run, which would be attributed to a loss of catalytic material during the recycling step.

Conclusion

In summary, we have developed a new aerobic oxidation system for the highly selective aerobic oxidation of HMF into FDCA using a magnetically separable [γ-Fe_2O_3@HAP-Pd(0)] catalyst. Several important parameters were studied, and it was found that the reaction temperature and base amount greatly affected HMF conversion and FDCA selectivity. Under the optimal conditions, high HMF conversion of 97.0% and FDCA yield of 92.9% were obtained after 6 h at 100 ^{o}C. Compared with other reported methods such as the use of supported Au nanoparticls as catalyst, our catalytic systems demonstrated two important advantages: (a) it only required the use of stoichiometric amount of base; (b) the catalyst showed high catalytic activity under atmospheric oxygen pressure even in the air. This method for the oxidation HMF into FDCA is in agreement with the viewpoint of green and sustainable chemistry. Notably, the superparamagnetic nature of the γ-Fe_2O_3@HAP-Pd(0) catalyst facilitates easy separation of the catalyst from reaction media by simply employing an external magnetic field. The catalyst can be successfully reused in five consecutive reaction runs, keeping its catalytic performance and selectivity. To our knowledge, this method is the first report on the selective aerobic oxidation of HMF into FDCA using magnetically separable catalysts by the use of stoichiometric amount of base under atmospheric oxygen in water. It is believed that this finding will be valuable for the production of useful chemicals from renewable resources and stimulate new areas in designing novel solid catalysts with high catalytic performance and recycling ability for chemical reactions, addressing economic and environmental issues.

Acknowledgements

The Project was supported by National Natural Science Foundation of China (No. 21203252), the Chenguang Youth Science and Technology Project of Wuhan City (No. 2014070404010212), and the Natural Science Foundation of Hubei Province (No. 2014CFB180).

References

1 R. A. Gross and B. Kalra, *Science*, 2002, 297, 803.
2 J. Q. Bond, D. M. Alonso, D. Wang, R. M. West and J. A. Dumesic, *Science*, 2010, **327**, 1110.
3 S. K. Tanneru and P. H. Steele, *Fuel*, 2014, **133**, 326.
4 Y. Roman-Leshkov, J. N. Chheda and J. A. Dumesic, *Science*, 2006, **213**, 1933.
5 N. Doassans-Carrere, J. H. Ferrasse, O. Boutin, G Mauviel and J. Lede, *Energ. Fuels*, 2014, **28**, 5103.
6 A. Ruppert, K. Weinberg and R. Palkovits, *Angew. Chem., Int. Ed.*, 2012, **51**, 2564.
7 A. Wang, and T. Zhang, *Acc. Chem. Res.*, 2013, **46**, 1377.
8 R. J. van Putten, J. C. van der Waal, E. de Jong, C. B. Rasrendra, H. J. Heeres, and J. G. de Vries, *Chem. Rev.*, 2013, **113**,1499.
9 J. J. Bozell and G. R. Petersen, *Green Chem.*, 2010, **12**, 539.
10 M. Besson, P. Gallezot and C. Pinel, *Chem. Rev.*, 2014, **114**, 1827-1870.
11 S. H. Xiao, B. Liu, Y. M. Wang, Z. F. Fang and Z. H. Zhang, *Bioresour. Technol.*, 2014, **151**, 361.
12 M. Zakrzewska, E. Bogel-Łukasik and R. Bogel-Łukasik, *Chem. Rev.*, 2011, **111**, 397.
13 Z. F. Fang, B. Liu, J. J. Luo, Y. S. Ren and Z. H. Zhang, *Biomass Bioenerg.*, 2014, **60**, 171-177.
14 Z.H. Zhang, B. Liu, K. L. Lv, J. Sun and K. J. Deng, *Green Chem.*, 2014, **16**, 2762.
15 B. Liu, Z.H. Zhang, K. L. Lv, K. J. Deng and H. M. Duan, *Appl. Catal. A: Gen.*, 2014, **472**, 64.
16 O. Casanova, S. Iborra and A. Corma, *ChemSusChem* 2009, **2**, 1138.
17 A. Corma, S. Iborra and A. Velty, *Chem. Rev.* 2007, **107**, 2411.
18 A. Gandini, A. J. D. Silvestre, C. P. Neto, A. F. Sousa and M. Gomes, *J. Polym. Sci., Part A: Polym. Chem.*, 2009, **47**, 295.
19 W. Partenheimer and V. V. Grushin, *Adv. Synth. Catal.*, 2001, **343**, 102.
20 B. Saha, S. Dutta, and M. M. Abu-Omar, *Catal. Sci. Technol.*, 2012, **2**, 79-81.
21 O. Casanova, S. Iborra and A. Corma, *ChemSusChem*, 2009, **2**, 1138.
22 S. E. Davis, B. N. Zope and R. J. Davis, *Green Chem*., 2012, **14**, 143.
23 J. Cai, H. Ma, J. Zhang, Q. Song, Z. Du, Y. Huang and J. Xu, *Chem. Eur. J*., 2013, **19**, 14215.
24 S. E. Davis, L. R. Houk, E. C. Tamargo, A. K. Datye and R. J. Davis, *Catal. Today*, 2011, **160**, 55.
25 L. Alamo-Nole, S. Bailon-Ruiz, T. Luna-Pineda, O. Perales-Perez, and F.R. Roman, *J. Mater. Chem. A*, 2013, **1**, 5509-5516.
26 T. Hara, T. Kaneta, K. Mori, T. Mitsudome, T. Mizugaki, K. Ebitani and K. Kaneda, *Green Chem.*, 2007, **9**, 1246.
27 M. Sheykhan, L. Ma'mani, A. Ebrahimi and A. Heydari, *J. Mol. Catal. A: Chem.*, 2011, **335**, 253.

28 Z.H. Zhang, Z.L. Yuan, D.G. Tang, Y.S. Ren, K.L. Lv and B. Liu, *ChemSusChem*, 2014, DOI: 10.1002/cssc.201402402 .
29 N. Jamwal, M. Gupta and S. Paul, *Green Chem*., 2008, **10**, 999.
30 K. Mori, T. Hara, T. Mizugaki, K. Ebitani and K. Kaneda, *J. Am. Chem. Soc*., 2004, 126, 10657.
31 N. Jamwal, M. Gupta and S. Paul, *Green Chem.*, 2008, **10**, 999.
32 L. Wang, J. L.Chen, V. Rudolph and Z. H. Zhu, *Adv. Powder Tech.* 2012, **23**, 465.
33 Z. C. Ma, H. Q. Yang, Y. Qin, Y. J. Hao and G. Li, Journal of Molecular Catalysis A: *J. Mol. Catal. A: Chem.* 2010, **331**, 78.
34 B. Liu, T. Huang, Z. H. Zhang, Z. Wang, Y. H. Zhang and J. L. Li, *Catal. Sci. Technol.* 2014, **4**, 1286.
35 C. Reichardt, Solvents and Solvent Effects in Organic Chemistry, third edition, Wiley-VCH Verlag GmbH & Co., Weinheim, 2003, p. 471.
36 R. R. Sever, and T. W. Root, *J. Phys. Chem. B*, 2003, **107**, 4080.
37 S. J. Ashcroft and M. B. Isa, *J. Chem. Eng. Data*, 1997, **42**, 1244.
38 H. A. Rass, N. Essayem and M. Besson, *Green Chem.*, 2013, **15**, 2240.
39 Y. Önal, S. Schimpf and P. Claus, *J. Catal.*, 2004, **223**, 122.
40 V. L. Snoeyink and D. Jenkins, Water Chemistry, Wiley and Sons, New York, Chichester, Brisbane, and Toronto, 1990, p. 462.
41 M. Crespo-Quesada, R. R. Dykeman, G. Laurenczy, P. J. Dyson and L. Kiwi-Minsker, *J. Catal.*, 2011, **279**, 66.
42 P. Lignier, S. Mangematin, F. Morfin, J. Rousset and V. Caps, *Catal. Today*, 2008, **138**, 50.

High yield of 2,5-furandicarboxylic acid was achieved from the aerobic oxidation of 5-hydroxymethylfurfural over a magnetic palladium nanocatalyst

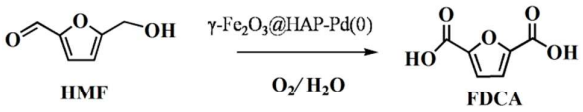

Conversion: 97%
Selectivity : 96%